arXiv:1405.3234v3 [quant-ph] 20 Sep 2014

Proposal for the generation of photon pairs with nonzero orbital angular momentum in a ring fiber

D. Javůrek,[1] **J. Svozilík,**[1,2,*] **J. Peřina Jr.**[3]

[1]*RCPTM, Joint Laboratory of Optics PU and IP AS CR, 17. listopadu 12, 771 46 Olomouc, Czech Republic*

[2]*ICFO-Institut de Ciències Fotòniques, Mediterranean Technology Park, Av. Carl Friedrich Gauss 3, 08860 Castelldefels, Barcelona, Spain*

[3]*Institute of Physics, Joint Laboratory of Optics PU and IP AS CR, 17. listopadu 50a, 771 46 Olomouc, Czech Republic*

[*]*jiri.svozilik@upol.cz*

Abstract: We present a method for the generation of correlated photon pairs in desired orbital-angular-momentum states using a non-linear silica ring fiber and spontaneous parametric down-conversion. Photon-pair emission under quasi-phase-matching conditions with quantum conversion efficiency 6×10^{-11} is found in a 1-m long fiber with a thermally induced $\chi^{(2)}$ nonlinearity in a ring-shaped core.

© 2014 Optical Society of America

OCIS codes: 060.2330,060.5565,190.4975

References and links

1. L. Allen, S. M. Barnett, and M. J. Padgett, *Optical AngularMomentum* (CRC Press, 2003).
2. J. P. Torres and L. Torner, *Twisted Photons: Applications of Light with Orbital Angular Momentum* (John Wiley & Sons, 2011).
3. N. Bozinovic, Y. Yue, Y. Ren, M. Tur, P. Kristensen, H. Huang, A. E. Willner, and S. Ramachandran, "Terabit-scale orbital angular momentum mode division multiplexing in fibers," Science **340**, 1545-1548 (2013).
4. G. Molina-Terriza, J. P. Torres, and L. Torner, "Twisted photons," Nature Physics **3**, 305-310 (2007).
5. G. Puentes, N. Hermosa, and J. P. Torres, "Weak measurements with orbital-angular-momentum pointer states," Phys. Rev. Lett. **109**, 040401 (2012).
6. M. Padgett and R. Bowman, "Tweezers with a twist," Nature Photonics **5**, 343-348 (2011).
7. P. Zhang, X.-F. Ren, X.-B. Zou, B.-H. Liu, Y.-F. Huang, and G.-C. Guo, "Demonstration of one-dimensional quantum random walks using orbital angular momentum of photons," Phys. Rev. A **75**, 052310 (2007).
8. A. Mair, A. Vaziri, G. Weihs, and A. Zeilinger, "Entanglement of the orbital angular momentum states of photons," Nature **412**, 313-316 (2001).
9. A. C. Dada, J. Leach, G. S. Buller, M. J. Padgett, and E. Andersson, "Experimental high-dimensional two-photon entanglement and violations of generalized bell inequalities," Nature Physics **7**, 677-680 (2011).
10. R. Fickler, R. Lapkiewicz, W. N. Plick, M. Krenn, C. Schaeff, S. Ramelow, and A. Zeilinger, "Quantum entanglement of high angular momenta," Science **338**, 640-643 (2012).
11. J. Svozilík, J. Peřina Jr., and J. P. Torres, "High spatial entanglement via chirped quasi-phase-matched optical parametric down-conversion," Phys. Rev. A **86**, 052318 (2012).
12. X. Li, P. L. Voss, J. E. Sharping, and P. Kumar, "Optical-fiber source of polarization-entangled photons in the 1550 nm telecom band," Phys. Rev. Lett. **94**, 053601 (2005).
13. J. Fulconis, O. Alibart, W. Wadsworth, P. Russell, and J. Rarity, "High brightness single mode source of correlated photon pairs using a photonic crystal fiber," Opt. Express **13**, 7572-7582 (2005).
14. J. Fan, A. Migdall, and L. Wang, "Efficient generation of correlated photon pairs in a microstructure fiber," Opt. Lett. **30**, 3368-3370 (2005).
15. R. A. Myers, N. Mukherjee, and S. R. J. Brueck, "Large second-order nonlinearity in poled fused silica," Opt. Lett. **16**, 1732-1734 (1991).

16. E. Y. Zhu, L. Qian, L. G. Helt, M. Liscidini, J. E. Sipe, C. Corbari, A. Canagasabey, M. Ibsen, and P. G. Kazansky, "Measurement of $\chi(2)$ symmetry in a poled fiber," Opt. Lett. **35**, 1530-1532 (2010).
17. G. Bonfrate, V. Pruneri, P. Kazansky, P. Tapster, and J. Rarity, "Parametric fluorescence in periodically poled silica fibers," Appl. Phys. Lett. **75**, 2356-2358 (1999).
18. K. P. Huy, A. T. Nguyen, E. Brainis, M. Haelterman, P. Emplit, C. Corbari, A. Canagasabey, P. G. Kazansky, O. Deparis, A. A. Fotiadi, P. Mégret, and S. Massar, "Photon pair source based on parametric fluorescence in periodically poled twin-hole silica fiber," Opt. Express **15**, 4419-4426 (2007).
19. E. Y. Zhu, Z. Tang, L. Qian, L. G. Helt, M. Liscidini, J. E. Sipe, C. Corbari, A. Canagasabey, M. Ibsen, and P. G. Kazansky, "Direct generation of polarization-entangled photon pairs in a poled fiber," Phys. Rev. Lett. **108**, 213902 (2012).
20. Y. Yue, Y. Yan, N. Ahmed, J.-Y. Yang, L. Zhang, Y. Ren, H. Huang, K. M. Birnbaum, B. I. Erkmen, S. Dolinar, M. Tur, and A. E. Willner, "Mode properties and propagation effects of optical orbital angular momentum (oam) modes in a ring fiber," IEEE Photonics J. **4**, 535-543 (2012).
21. A. Canagasabey, C. Corbari, A. V. Gladyshev, F. Liegeois, S. Guillemet, Y. Hernandez, M. V. Yashkov, A. Kosolapov, E. M. Dianov, M. Ibsen, and P. G. Kazansky, "High-average-power second-harmonic generation from periodically poled silica fibers," Opt. Lett. **34**, 2483-2485 (2009).
22. A. W. Snyder and J. Love, *Optical Waveguide Theory*, (Springer, 1983).
23. V. Brückner, *Elements of Optical Networking* (Springer, 2011).
24. M. J. Collins, C. Xiong, I. H. Rey, T. D. Vo, J. He, S. Shahnia, B. J. Eggleton,(2013). *Integrated spatial multiplexing of heralded single-photon sources*, Nat. Commun. **4**, 1-7 (2013).

1. Introduction

Optical fields with non-zero orbital angular momentum (OAM), which show a non-gaussian transverse amplitude and phase profiles [1, 2], are of great interest in a myriad of scientific and technological applications, such as secure communications [3], ultra-precise measurements [4, 5], nano-particle manipulation [6] or quantum computing [7]. These applications push forward the development of new methods aimed at the preparation of optical fields with OAM in both the classical and quantum (i.e. single-photon) regimes.

Paired photons with nonzero OAM are widely generated nowadays via the nonlinear optical process of spontaneous parametric down-conversion (SPDC), where photons are generated in pairs (signal and idler). Such paired photons can show quantum correlations (entanglement) in several degrees of freedom including polarization, frequency, or momentum. Entanglement may occur also in the OAM degree of freedom [8], as experimentally demonstrated in [9]. States with the winding numbers around 300 have already been observed in volume optics [10]. Dimensions of this entanglement reaching even 10^5 are theoretically predicted in [11]. However, the generation of OAM entanglement in optical fibers still represents a challenge, which solution could open the door for many applications that would benefit from using guided modes (low losses in optical elements, long transmission distances). Recently, guided OAM states in fibers with the winding numbers up to 1 have been observed [3].

There are mainly two problems to overcome. On the one hand, the presence of inverse symmetry in ideally cylindrically-shaped silicon optical fibers excludes the existence of $\chi^{(2)}$ nonlinearity. For this reason, photon pairs in optical fibers are generally generated by means of an alternative nonlinear process (four-wave mixing) which utilizes instead the third-order nonlinearity of silicon [12–14]. Small values of the elements of $\chi^{(3)}$ nonlinear tensor can be compensated by increasing the interaction length to give higher photon-pair fluxes. Unfortunately, this is accompanied by equal enhancement of other effects, i.e., Raman scattering, that cause unwanted higher noise contributions to the generated flux. Nevertheless, silicon optical fibers can become nonlinear using the method of thermal poling [15, 16] which provides a nonzero $\chi^{(2)}$ susceptibility and also enables to employ quasi-phase-matching (QPM) reached via UV erasure [17–19].

On the other hand, the propagation of photons with OAM in the usual step-index long optical fibers do not prevent cross-talk among modes with different OAM from being strong, which results in the fast deterioration of the purity of the OAM propagating modes. However, modern

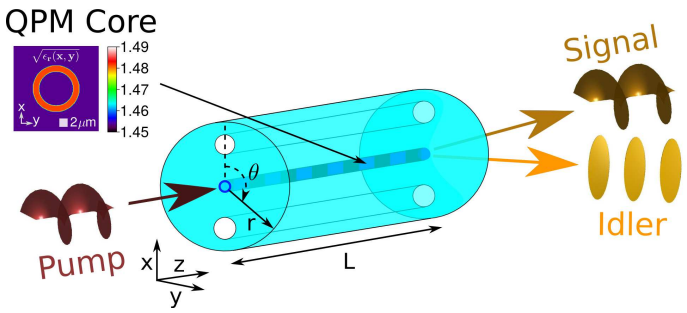

Fig. 1. Sketch of the proposed silica fiber with a ring-shaped core utilizing quasi-phase-matching as a source of entangled photon pairs. The inset represents the transverse profile of refraction index $\sqrt{\varepsilon_r(x,y)}$ at the pump wavelength $\lambda_{p0} = 0.775\,\mu m$.

technology suggest also a solution in the form of ring and vortex fibers with ring-shaped cores [20] that are more resistant against cross-talk. Here, we show that entangled photon pairs in OAM modes can be generated in this type of silica fiber with thermal poling.

2. Theoretical model

The profile of the fiber with a ring-shaped core considered here is shown in Fig. 1. As the optical fields of guided modes are localized in the close vicinity of the core [20,21], the resulting radial symmetry considerably simplifies their determination via the Maxwell equations. In a real fiber, weak anisotropy occurs due to non-homogenity and stress in the material caused by two holes far away from the ring core that serve for poling wires [16]. Comparison of analytical results with the precise ones obtained by the full-vector mode solver from *Lumerical* has revealed that the applied model is appropriate as long as the elements ε_x and ε_y of linear permittivity satisfy the condition $\sqrt{\varepsilon_y/\varepsilon_x} - 1 < 1 \times 10^{-7}$.

In rotationally symmetric systems, the full electric (**E**) and magnetic (**H**) fields can be derived from their longitudinal components E_z and H_z. Moreover, they can be written as the product of a function that depends only on the azimuthal coordinate (θ), and an another function that depends only on the radial coordinate (r), i.e., $E_z, H_z \sim f(r)g(\theta)\exp[i(\beta z - \omega t)]$. Functions $f(r)$ and $g(\theta)$ describe spatial profiles of fields along the radial and azimuthal directions, respectively. They satisfy the eigenvalue equations:

$$r^2\frac{\mathrm{d}^2 f(r)}{\mathrm{d}r^2} + r\frac{\mathrm{d}f(r)}{\mathrm{d}r} + r^2\left[\frac{\omega^2\varepsilon_r}{c^2} - \beta^2 - \frac{n^2}{r^2}\right] f(r) = 0, \qquad \frac{\mathrm{d}^2 g(\theta)}{\mathrm{d}\theta^2} + n^2 g(\theta) = 0, \tag{1}$$

where β is the propagation constant (eigenvalue) of a guided mode with frequency ω; c denotes the velocity of light in the vacuum and ε_r means the relative dielectric permittivity. Transverse profile of $\sqrt{\varepsilon_r}$ is shown in the inset of Fig. 1. To simplify our calculations, we consider ε_r only as a scalar-function. Integer number n counts eigenmodes that are solutions of the second equation in (1) describing azimuthal properties of optical fields. These solutions have the form of harmonic functions with frequencies determined by n. On the other hand, solutions of the first equation in (1) for a fixed value n are expressed in terms of the Bessel functions. For fixed values of frequency ω and index n, the continuity requirements on core boundaries admit only a discrete set of eigenmodes with suitable values of propagation constants β [22]. If we take into account field polarizations, we reveal the usual guided modes of optical fibers that are appropriate also for describing photon pairs. Spatial modes characterized by an OAM (winding) number l are then obtained as suitable linear combinations of the above fiber eigenmodes $\mathbf{e}_\eta(\omega)$

classified by multi-index η that includes azimuthal number n, radial index of solutions of the first equation in (1) and polarization.

On quantum level, the nonlinear process of SPDC converts a pump photon into a photon pair described by a first-order perturbation solution of the Schrödinger equation with interaction nonlinear Hamiltonian $\hat{H}_I$ written in the radial coordinates as follows:

$$\hat{H}_I(t) = 2\varepsilon_0 \int_{S_\perp} r dr d\theta \int_{-L}^{0} dz\, \chi^{(2)}(z) : \mathbf{E}_p^{(+)}(r,\theta,z,t)\hat{\mathbf{E}}_s^{(-)}(r,\theta,z,t)\hat{\mathbf{E}}_i^{(-)}(r,\theta,z,t) + \text{h.c.} \quad (2)$$

In Eq. (2), subscripts p, s and i denote in turn the pump, signal and idler fields. Symbol : is tensor shorthand with respect to three indices of $\chi^{(2)}$ tensor and ε_0 denotes the vacuum permittivity and h.c. replaces the Hermitian conjugated term. Symbol $S_\perp$ means the transverse area of the fiber of length L. Effectively induced nonlinear susceptibility $\chi^{(2)}$ has the following non-zero elements: $\chi^{(2)}_{xxx} \simeq 3\chi^{(2)}_{xyy}$ and $\chi^{(2)}_{xyy} = \chi^{(2)}_{yxx} = \chi^{(2)}_{yxy} = 0.021$ pm/V [16]. We note that small variations in the $\chi^{(2)}$ profile across the core are effectively smoothed out by the nonlinear interaction [see Eq. (6) below]. The fiber is pumped by a strong (classical) pump beam which positive-frequency part $\mathbf{E}_p^{(+)}$ of the electric-field amplitude can be decomposed into the above introduced eigenmodes $\mathbf{e}_{p,\eta_p}(\omega_p)$ as:

$$\mathbf{E}_p^{(+)}(r,\theta,z,t) \;=\; \sum_{\eta_p} A_{p,\eta_p} \int d\omega_p\, \mathscr{E}_p(\omega_p)\mathbf{e}_{p,\eta_p}(r,\theta,\omega_p) \exp\left(i[\beta_{p,\eta_p}(\omega_p)z - \omega_p t]\right). \quad (3)$$

In Eq. (3), A_{p,η_p} gives the amplitude of mode η_p and $\mathscr{E}_p$ denotes the normalized pump amplitude spectrum. Similarly, the negative-frequency parts $\hat{\mathbf{E}}_s^{(-)}$ and $\hat{\mathbf{E}}_i^{(-)}$ of the signal and idler electric-field operators can be written as:

$$\hat{\mathbf{E}}_a^{(-)}(r,\theta,z,t) = \sum_{\eta_a} \int d\omega_a \sqrt{\frac{\hbar\omega_a}{4\pi\varepsilon_0 \bar{n}_a c}}\, \hat{a}^\dagger_{a,\eta_a}(\omega_a)\mathbf{e}^*_{a,\eta_a}(r,\theta,\omega_a) \exp\left(i[\beta_{a,\eta_a}(\omega_a)z - \omega_a t]\right), \quad (4)$$

$a = s,i$ and $\hbar$ is the reduced Planck constant. Symbol $\bar{n}_a$ stands for an effective refractive index of field a. The creation operators $\hat{a}^\dagger_{a,\eta_a}(\omega_a)$ give a photon into field a with multi-index η_a and frequency ω_a.

The state $|\psi\rangle$ describing a photon pair at the output plane of the fiber can be written as a quantum superposition comprising states of all possible eigenmode combinations (η_s,η_i):

$$\begin{aligned} |\psi\rangle \;=\; & -\frac{i}{c} \sum_{\eta_s,\eta_i} \sum_{\eta_p} A_{p,\eta_p} \int d\omega_s \int d\omega_i \sqrt{\frac{\omega_s\omega_i}{\bar{n}_s\bar{n}_i}}\, \mathscr{E}_p(\omega_s+\omega_i) \\ & \times I_{\eta_p,\eta_s\eta_i}(\omega_s,\omega_i)\hat{a}^\dagger_{s,\eta_s}(\omega_s)\hat{a}^\dagger_{i,\eta_i}(\omega_i)|\text{vac}\rangle; \end{aligned} \quad (5)$$

$|\text{vac}\rangle$ is the initial signal and idler vacuum state. Function $I_{\eta_p,\eta_s\eta_i}(\omega_s,\omega_i)$ quantifies the strength of interaction among the indicated modes at the given signal and idler frequencies,

$$\begin{aligned} I_{\eta_p,\eta_s\eta_i}(\omega_s,\omega_i) \;=\; & \int_{S_\perp} r dr d\theta \int_{-L}^{0} dz\, \chi^{(2)}(z) : \mathbf{e}_{p,\eta_p}(r,\theta,\omega_s+\omega_i)\mathbf{e}^*_{s,\eta_s}(r,\theta,\omega_s)\mathbf{e}^*_{i,\eta_i}(r,\theta,\omega_i) \\ & \times \exp[i\Delta\beta_{\eta_p,\eta_s\eta_i}(\omega_s,\omega_i)z]; \end{aligned} \quad (6)$$

$\Delta\beta_{\eta_p,\eta_s\eta_i}(\omega_s,\omega_i) \equiv \beta_{p,\eta_p}(\omega_s+\omega_i) - \beta_{s,\eta_s}(\omega_s) - \beta_{i,\eta_i}(\omega_i)$ characterizes phase mismatch of the nonlinear interaction among individual modes.

Using the state $|\psi\rangle$ in Eq. (5), a signal photon-number density $n_{\eta_s}(\omega_s)$ observed in mode η_s is computed along the formula

$$n_{\eta_s}(\omega_s) \;=\; \sum_{\eta_i} \int d\omega_i \langle\psi|\hat{a}^\dagger_{s,\eta_s}(\omega_s)\hat{a}^\dagger_{i,\eta_i}(\omega_i)\hat{a}_{s,\eta_s}(\omega_s)\hat{a}_{i,\eta_i}(\omega_i)|\psi\rangle. \quad (7)$$

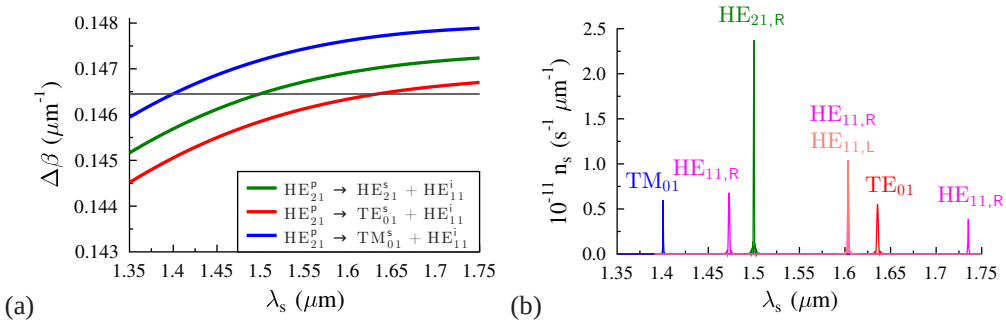

Fig. 2. (a) Phase mismatch $\Delta\beta_{\eta_p,\eta_s\eta_i}$ as it depends on signal wavelength λ_s for three different combinations of eigenmodes fulfilling the OAM selection rule. The horizontal grey line indicates the maximum of spatial spectrum of $\chi^{(2)}$ modulation expressed in $-\Delta\beta$. The period of modulation $\Lambda = 42.9$ μm is chosen such that quasi-phase-matching occurs for $\lambda_{s0} = 1.5$ μm and process $\mathrm{HE}^{\mathrm{p}}_{21,\mathrm{R}} \rightarrow \mathrm{HE}^{\mathrm{s}}_{21,\mathrm{R}}, +\mathrm{HE}^{\mathrm{i}}_{11,\mathrm{R}}$. (b) Signal photon-number density n_{η_s} as a function of signal wavelength λ_s for a 1 m-long fiber with period $\Lambda = 42.9$ μm. Different modes recognized in the signal field are indicated.

3. Numerical results

In the analysis, we consider a silica fiber with a ring-shaped core created by doping the base material with 19.3 mol% of GeO_2 (for details, see [23]). The SPDC process is pumped by a monochromatic beam of wavelength $\lambda_{p0} = 0.775$ μm. The fiber was designed such that photon pairs are emitted around the wavelength 1.550 μm used in fiber communication systems. A right-handed circularly polarized $\mathrm{HE}^{p}_{21,R}$ mode with OAM number $l = 1$ (composed of $\mathrm{HE}_{21,\mathrm{odd}}$ and $\mathrm{HE}_{21,\mathrm{even}}$ modes, see [22]) has been found suitable for the pump beam. It gives minimal crosstalk with other pump modes (namely TM_{01}) at the given wavelength. Importantly, according to the full-vector numerical model, the propagation constants of eigenmodes $\mathrm{HE}_{21,\mathrm{odd}}$ and $\mathrm{HE}_{21,\mathrm{even}}$ for pump (signal) field differ only by 3.88×10^{-3} (1.14×10^{-3}) rad/m in an anisotropic fiber with $\sqrt{\varepsilon_y/\varepsilon_x} - 1 = 1\times10^{-7}$. The generated signal and idler photons fulfil the energy conservation law ($\omega_p = \omega_s + \omega_i$) and also the selection rule for OAM numbers ($l_{\eta_p} = l_{\eta_s} + l_{\eta_i}$) that originates in the radial symmetry of the nonlinear interaction. Under these conditions, efficient photon-pair generation has been found for a signal photon in mode $\mathrm{HE}^{s}_{21,R}$ ($l_s = 1$) and an idler photon in mode $\mathrm{HE}^{i}_{11,R}$ or $\mathrm{HE}^{i}_{11,L}$ ($l_i = 0$) which represent the right- and left-handed polarization variants of the same spatial mode. As the phase-matching curves in Fig. 2(a) show, also other efficient combinations of signal and idler modes are possible, namely $\mathrm{HE}^{p}_{21,R} \rightarrow \mathrm{TE}^{s}_{01} + \mathrm{HE}^{i}_{11}$ and $\mathrm{HE}^{p}_{21,R} \rightarrow \mathrm{TM}^{s}_{01} + \mathrm{HE}^{i}_{11}$.

However, QPM reached via the periodic modulation of $\chi^{(2)}$ nonlinearity allows to separate different processes. The right choice of period Λ of $\chi^{(2)}$ nonlinearity tunes the desired process that is exclusively selected provided that the $\chi^{(2)}$ spatial spectrum is sufficiently narrow. For our fiber, the $\chi^{(2)}$ spatial spectrum has to be narrower than 1×10^{-3} $\mu\mathrm{m}^{-1}$. This is achieved in general for fibers longer than 1 cm. The analyzed fiber 1 m long with the width of spatial spectrum equal to 7.6×10^{-6} $\mu\mathrm{m}^{-1}$ allows to separate the desired process from the other ones with the precision better than 1:100.

According to Fig. 2(b) the greatest values of signal photon-number density n_{s,η_s} occur for mode $\mathrm{HE}^{s}_{21,R}$ with an OAM number $l = +1$ around the wavelength $\lambda_s = 1.5$ μm. The full width at the half of maximum of the peak equals $\Delta\lambda_s = 0.96$ nm. The second largest contribution belongs to the processes involving modes $\mathrm{HE}^{s}_{11,R}$ and $\mathrm{HE}^{s}_{11,L}$ that interact with mode $\mathrm{HE}_{21,R}$. They build a common peak found at the wavelength $\lambda_s = 1.603$ μm. In signal photon-number

density n_{s,η_s}, there also exists two peaks of mode $\mathrm{HE}^s_{11,R}$ that form pairs with the peaks created by modes TM_{01} and TE_{01}. These peaks are shifted towards lower and larger wavelengths, respectively, due to their propagation constants. Whereas the peak belonging to mode TM^s_{01} occurs at the lower wavelength $\lambda = 1.4\ \mu$m, the peak given by mode TE^s_{01} is located at the longer wavelength $\lambda = 1.635\ \mu$m. Spectral shifts of these peaks allow their efficient separation by frequency filtering. The generated photon-pair field is then left in the state with a signal photon in mode $\mathrm{HE}^s_{21,R}$ and an idler photon either in state $\mathrm{HE}^i_{11,R}$ or $\mathrm{HE}^i_{11,L}$. The weights of both possible idler states $\mathrm{HE}^i_{11,R}$ and $\mathrm{HE}^i_{11,L}$ in quantum superposition are the same which gives linear polarization of the overall idler field. Also, pump-field leakage into modes TE^p_{01} and TM^p_{01} caused by imperfect fiber coupling may occur. This gives extra peaks in the signal photon-number density n_{s,η_r} that are spectrally separated from those discussed above by 15 nm.

The fiber 1 m long provides around 240 photon pairs per 1 s and 1 μW of pumping in the analyzed modes. For comparison, the fibre 10-cm long generates around 20 photon pairs per 1 s and 1 μW of pumping in the same configuration. This means that a slightly better than linear increase of photon-pair numbers with the fiber length occurs. Strong correlations between the signal and idler frequencies result in fast temporal correlations between the signal and idler detection times occurring in a time window 7 ps long. We notice, that the process can also be considered in its left-handed polarization variant in which the pump beam propagates as a $\mathrm{HE}_{21,L}$ mode. Both variants provide photon pairs suitable, e.g., for quantum metrology or heralded single-photon sources [24] giving Fock states with non-zero OAM numbers.

Quasi-phase matching allows also other efficient combinations of modes. For example, the pump beam in mode $\mathrm{HE}^p_{11,R}$ (or $\mathrm{HE}^p_{11,L}$) with $l_p = 0$ provides spectrally broad-band SPDC that may give photon pairs with temporal correlations at fs time-scale. Also photon pairs entangled in OAM numbers can be obtained in this configuration in which the signal (idler) photon propagates either as HE^s_{21R} (HE^i_{21L}) mode or HE^s_{21L} (HE^i_{21R}). We note that vortex fibers [3] are also suitable for SPDC as they provide similar conditions for photon-pair generation as the analyzed ring fibers. Moreover, their additional core gives better stability to fundamental modes participating in the nonlinear interaction. Both ring and vortex fibers thus have a large potential to serve as versatile fiber sources of photon pairs in OAM states useful in optical information processing.

4. Conclusion

A ring fiber with thermally induced $\chi^{(2)}$ nonlinearity and periodical poling has been presented as a promising source of photon pairs being in eigenmodes of orbital angular momentum. Spontaneous parametric down-conversion has been pumped by a beam with nonzero orbital angular momentum that has been transferred into one of the down-converted beams. Several mutually competing nonlinear processes exploiting different modes can be spectrally separated. Other configurations also allow for the emission of spectrally broad-band photon pairs as well as photon pairs entangled in orbital-angular-momentum numbers. This makes the analyzed ring fiber useful for many integrated fiber-based applications.

Acknowledgments

The authors thank J.P. Torres for his advice and useful comments. D.J. acknowledges J.P. Torres for his support at ICFO. Support by projects CZ.1.05/2.1.00/03.0058 and CZ.1.07/2.3.00/20.0017 of MŠMT ČR and P205/12/0382 of GA ČR are acknowledged. D.J. and J.P. thanks the project PrF_2013_006 of IGA UP Olomouc. J.S. thanks the projects CZ.1.07/2.3.00/30.0004 and CZ.1.07/2.3.00/20.0058 of MŠMT ČR.